A Comparative Study of Predictive Methods for Liquefaction Induced Embankment Displacements

Geoffrey R. Martin[1] and Ping Qiu[2]

ABSTRACT

Many bridge failures in past earthquakes have resulted from large post liquefaction lateral deformations of bridge approach fills. In considering the problem of retrofit of existing bridges where liquefiable foundation soils are found, there is a clear need to develop improved predictive methods for post liquefaction deformations of approach fills, prior to the investment of heavy costs related to ground remediation. In this presentation, current design approaches for evaluating post liquefaction lateral deformations are compared by utilizing the simple problem of a thirty-foot high approach fill on a liquefiable sand stratum. The comparative approaches encompass simplified one-dimensional Newmark sliding block analyses and more complex two-dimensional finite difference models. The comparative studies indicate that simplified one-dimensional Newmark sliding block analyses can provide a practical basis for less conservative retrofit design, provided the time at which residual strength is initiated when liquefaction occurs and the effects of initial static shearing stresses are taken into account.

[1] Professor and Chairman, Department of Civil Engineering, University of Southern California, Los Angeles.
[2] Graduate Student, Department of Civil Engineering, University of Southern California, Los Angeles

INTRODUCTION

In the 1964 Alaska and Niigata earthquakes, liquefaction induced lateral embankment or approach fill deformations were particularly destructive to highway and railway bridges (Bartlett and Youd, 1992). Ninety-two highway bridges in Alaska were severely damaged or destroyed and a further forty-nine bridges received moderate to light damage. Liquefaction induced lateral deformations of embankments have caused similar bridge damage in many more recent earthquakes including those in Japan, Puerto Rico, and the Philippines. Clearly this is a problem that needs to be addressed during the seismic design of bridges in liquefaction prone environments. In the case of the seismic retrofit of existing bridges, however, it is desirable to reduce any conservatism in assessing the magnitude of post liquefaction deformations, prior to the investment of heavy costs related to ground remediation.

In this presentation, differences in lateral displacement predictive methods are examined by utilizing the simple problem of a thirty-foot high approach fill on a liquefiable sand stratum. By examining the assumptions used and comparing displacement predictions, both the sensitivity of analysis methods and inherent conservatism may be assessed.

To simulate the observed failure mode of approach fills in past earthquakes for comparative analytical studies, we have idealized the problem as shown in Fig. 1. The figure is representative of a compacted earth approach fill located above a liquefiable foundation layer. From a vulnerability standpoint, the question arises as to the magnitude of lateral embankment displacement which could be induced during the earthquake adopted for seismic retrofit. A reliable estimate of this displacement would allow evaluation of the vulnerability of the existing bridge to such deformation.

For practical reasons, the Newmark Sliding Block approach for computing earthquake induced embankment displacements (Newmark, 1959) is generally adopted in practice. A common conservative approach to the problem is to assume that a liquefied soil layer mobilizes a residual undrained strength s_{ur} following liquefaction, with the value of s_{ur} determined by correlation with standard penetration blow counts or from laboratory tests. Using limiting equilibrium principles, a horizontal yield acceleration coefficient k_y leading to a factor of safety of one for the most critical sliding block is then determined. Assuming rigid block response, the ground motions which will lead to incremental horizontal block displacements when $k > k_y$, may be represented by the acceleration time history at the base of the sliding block. Assuming residual strength is mobilized at time zero during earthquake loading, the resulting block displacement may be computed for a given time history through use of a simple computer program. Alternatively, non-dimensional

charts may be used, expressing permanent displacements as a function of k_y/k_{max}, where k_{max} is the maximum ground acceleration coefficient.

Research studies to date have examined the assumptions used for the simplified Newmark approach described above with a view to understanding the mechanisms of failure and reducing potential conservatism. The results of these studies are briefly summarized below and illustrate the following aspect of the problem:

- The sensitivity of displacements to input ground motions.
- The time history of pore pressure build up leading to the point at which residual strength should be triggered for analyses.
- The potential influence of horizontal static shearing stresses beneath embankment slopes and their role in the impeding the rate of excess pore pressure build up.
- The use of two-dimensional non-linear response analyses to simulate the embankment displacement mechanism.
- Comparative evaluation of assumptions on displacement predictions.

DISPLACEMENT SENSITIVITY TO INPUT MOTIONS

Embankment displacements predicted by the Newmark Sliding Block model are primarily a function of k_y/k_{max}, peak ground velocity V and peak ground acceleration A. The number of load cycles exceeding yield as reflected by the earthquake magnitude M, could also be a factor. A number of analytical studies to determine displacements as a function of k_y/k_{max} have been made using a variety of earthquake records. However, many of the available displacement charts have been normalized by scaling earthquake records to peak accelerations of 0.5g and peak velocities of 30 inches per second.

To develop a more convenient design chart and to investigate the range of variability of predictive displacements, a study was made using the database published by Hynes and Franklin (1985), where displacements computed using a large number of earthquake records have been documented. For this study, the data was limited to earthquakes with a magnitude range of 6.0 to 7.5. For the purpose of data analysis an equation of the form:

$$d = C\,(k_y/k_{max})^{a1}\,(1 - k_y/k_{max})^{a2}\,A^{a3}\,V^{a4}\,M^{a5}$$

was used. Regression analyses indicated that earthquake magnitude does not have major effect on predictions and that a equation of the form:

$$d = 6.82 (k_y/k_{max})^{-0.55} (1 - k_y/k_{max})^{5.08} A^{-0.86} V^{1.66}$$

describes the mean displacement with an R^2 error of 0.9247. In the above equation a consistent set of units of inches, and seconds are used. By normalizing the displacement by a factor $A^{-.86} V^{1.66}$, a normalized displacement chart showing $d/ A^{-.86} V^{1.66}$ vs. k_y/k_{max} may be plotted and is shown in Fig. 2. Almost 80% of all data fall on a narrow band leading to the nominal upper and lower bounds as shown. Upper bound displacements are about twice those of the mean, while lower bound values are about one quarter of the mean.

TIME HISTORY OF PORE PRESSURE BUILD UP

To pursue analytical studies addressing questions related to the time history of pore pressure build up and two-dimensional response, the idealized embankment configuration and the material properties shown in Fig 3 were assumed. To study the effects of liquefaction we focused on layer 1 by assuming a low relative of density of 40%. The cohesionless materials in the idealized embankment were assumed to be those of Nevada sand which was used for the VELACS Project (Arulmoli et.al., 1992). Penetration blow counts in $(N_1)_{60} = 8$ and $(N_1)_{60} = 16$ were assumed for layers 1 and 2 respectively. An undrained residual strength of 200 psf was chosen for layer 1 from the standard relationships shown in Fig. 4. Pore pressure build up was suppressed in the lower layer 2 to ensure a dominant lateral sliding mechanism. The 1940 El Centro earthquake with a peak ground acceleration of 0.33g was input at bedrock level.

Time history of pore pressure increases were computed for one-dimensional free field conditions represented by column 1 and column 2, using the effective stress response program DESRA (Lee and Finn, 1978). Modifications to this program were made to make it more user friendly in a practical sense. These modifications included the use of a simplified two-parameter pore pressure model suggested by Byrne (1991) and a generalized non-linear backbone curve with automatic generation of parameters to represent a given curve describing variations in shear modulus with shear strain amplitude. The two pore pressure parameters were selected to match a standard liquefaction strength curve developed from field blow count data and a design earthquake magnitude. The simplifications make the program more amenable to routine design practice. An Iwan model (1967) was used as a non-linear constitutive model and incorporates an array of elasto-plastic elements which simulate a given non-linear backbone curve and provides hysteretic

damping. This physically based mechanistic model provides a good simulation of permanent displacement induced by soil yield.

Fig. 5 shows the G/G_{max} vs. shear strain amplitude curve assumed for analyses and the liquefaction strength curve for layer 1. In the program DESRA, G_{max} values were assigned to layer properties using the equation: $G_{max} = 20000(N_1)_{60}^{1/3}(\sigma'_m)^{1/2}$, where $(\sigma'_m)^{1/2}$ is the mean effective stress. A non-linear backbone or shear stress-shear strain curve was then constructed to be compatible with the G/G_{max} vs. γ curve. The backbone curve was then used to fix the Iwan model parameters, which in turn define the soil behavior under cyclic loading. The field liquefaction strength curve for layer 1 was constructed to be compatible with the assumed blowcount $(N_1)_{60} = 8$. The difference in the two curves shown reflect the effect of initial confining stresses.

The results of the DESRA analyses with respect to pore pressure build up are shown in Fig. 6. For column 1, the loose sand layer 1 liquefied after about two seconds of strong shaking. The corresponding large shearing strains occurring in the layer are interpreted as relative displacements of the soil column above the liquefied layer in Fig. 6a. These displacements can be considered to reflect ground lurch leading to a permanent displacement of the ground of about 0.25 feet. For column 2, liquefaction occurred after about three seconds leading to permanent lurch displacements of the soil column above the liquefied layer of about 0.3 feet. Note the significant reductions in surface accelerations compared to input accelerations. The low 0.05g peak acceleration reflects the limiting inertial loads which can be carried by the upper soil column following mobilization of the post liquefaction residual strength of 200 psf. in layer 1. The shear stress vs. shear strain time history (0 - 4 seconds) for layer 1 (column 2) is shown in Fig. 7.

TWO-DIMENSIONAL RESPONSE ANALYSES

To study the effects of two-dimensional earthquake response on the mechanisms of lateral deformation of the slope and to evaluate the influence of initial static shearing stresses beneath the sloping embankment on liquefaction resistance, a two-dimensional dynamic response program TENSI was used. The program TENSI has been documented by Larkin et.al.,(1991). TENSI is a non-linear two-dimensional total stress response analysis program utilizing a multiple yielding surface model to simulate non-linear soil behavior. The latter model has been described by Iwan (1967), and is a kinematic strain hardening model analogous to the model used for the one-dimensional analyses described above. The original program TENSI has been modified to form

TENSI-M to allow inclusion of the effects of initial static stresses due to embankment construction on the earthquake response. The program is now divided into two parts: static analysis and dynamic analysis. In the static analysis, gravity loading is used to simulate the construction procedure, where the embankment is built in a sequence of layers. For each loading layer, the program runs twice. The first run is under an assumption that loosely placed soil has only very small stiffness, that is, a very low modulus. In the second run, the stiffness matrix is formed using compacted soil modulus values, but resetting displacements and strains from the first run, that is, the position after settlement of loose soil is chosen as a reference position. A Gaussian procedure is used to solve for displacements from layer gravity loading. The embankment shown in Fig. 3 is assumed to be constructed in three layers. The resulting static shear stress distribution over layer 1 is shown in Fig. 8. The highest shear stresses occur beneath the slope, leading to an average ratio of horizontal static shearing stress to initial vertical effective stress beneath the slope of about 0.25. The static shear stress will affect liquefaction strength as described by Vaid and Finn (1979) and will be discussed further below.

As a two-dimensional effective stress constitutive model has yet to be programmed into TENSI-M, in order to study the two-dimensional mechanisms of lateral deformation, the shear modulus and shear strength of the loose sand layer were progressively degraded from initial values to residual values using the average increases in pore pressure from the one-dimensional DESRA analyses. The TENSI-M results at the vertical free field boundaries, columns 1 and 2, are compared to the results from DESRA in Fig. 9. The TENSI-M results are very similar to the DESRA results except for permanent lurch displacements which are about 0.6 feet. This increase may be attributed to the effects of initial static horizontal shearing stresses that extend out as far as column 1.

The displacement pattern as a whole for the TENSI-M analyses, is shown in Fig. 10. The horizontal sliding mode of the embankment is clearly indicated with evidence of passive failure a the toe. The time history of average horizontal slope displacement is shown in Fig. 12.

CALCULATION OF EMBANKMENT DISPLACEMENTS USING THE NEWMARK METHOD

To perform conventional Newmark analyses, it is necessary to first determine the critical sliding block and the corresponding yield acceleration (assuming the residual strength of 200 psf is mobilized in layer 1) using conventional pseudostatic limiting equilibrium methods. The position of the critical sliding block is roughly that shown in Fig. 1. The corresponding yield acceleration is 0.03g. The static factor of safety is 1.15 which provides for static stability under post

liquefaction conditions, that is, a flow failure would not occur. Horizontal displacements of the block induced by the input earthquake acceleration time history were computed using the program DISPLMT (Houston et.al., 1987). The time histories of displacement assuming residual strength triggered following liquefaction either at time = 0 or 2 seconds are shown in Fig. 12, leading to maximum displacements of about 2.8 and 2.5 feet respectively. If liquefaction had not occurred until after about 4 or 5 seconds of strong shaking, the reductions in maximum displacement from the assumption of triggering at t = 0 would have been more significant. A block displacement of about 2 feet was computed from the mean curve shown in Fig. 2, using the average maximum V and A at the base of the liquefied layer from DESRA results. The corresponding upper bound displacement is about 4 feet. The maximum displacement from TENSI-M analyses assuming residual strengths triggered at 2 seconds, is about 3.3 feet.

The embankment displacement estimates assume pore pressure generation under one-dimensional free field conditions and do not reflect the influence of static shearing stress reducing the rate of pore pressure build up. The latter effects were taken into account by utilizing the results of published laboratory data, where simple shear test were conducted with varying initial static shearing stress ratios, as reported by Vaid and Finn (1979), as shown for example in Fig. 11. By modifying the liquefaction strength curve beneath the sloping embankment to account for an average static shearing stress ratio of 0.25, (a liquefaction strength increase of about 25%), it was found that the earthquake induced pore pressure increases reached only about 40% of the values required to induce liquefaction. The effect of reduced strength degradation beneath the sloping embankment to values corresponding to 40% of the difference between static strengths and residual strengths significantly increased the yield accelerations and reduced displacement. The displacement time histories are shown plotted on Fig. 12 and resulted in a maximum of about 0.2 feet of displacement.

SUMMARY AND CONCLUSIONS

From the above sensitivity study it is clear that both the point of time during the earthquake when residual strength is triggered by liquefaction and the effects of initial static shearing stresses in reducing the rate of pore pressure build up, have a major influence on the magnitude of earthquake induced post liquefaction displacements. However, research to date has indicated that the Newmark approach for evaluating post liquefaction embankment deformations can provide a practical basis for design provided the above effects are taken into account. Through on-going research exploring the sensitivity of displacements to the above variables, it is anticipated that simplified final design approaches and charts can be documented for routine use in the field. Additional centrifuge tests as part of an RPI research program will include experiments where

embankment deformations will be measured utilizing a model configuration similar to that shown in Fig. 1. These tests will provide additional verification for the analysis approach.

ACKNOWLEDGMENTS:

The research described above was supported by the National Center for Earthquake Engineering Research Highway Project, funded by the Federal Highway Administration.

REFERENCES

Arulmoli, K, Muraleetharan, K. K., Hossain, M. M. and Fruth, L. S., (1992): "VELACS, Verification of Liquefaction Analysis By Centrifuge Studies Laboratory Testing Program, Soil Data Report", The Earth Technology Corporation, California, Earth Technology Project No. 90-0562.

Bartlett, Steven F. and Youd , T. Leslie, (1992): "Case Histories of Lateral Spreads Caused by the 1964 Alaska Earthquake", Case Studies of Liquefaction and Lifeline Performance During Past Earthquakes, Vol. 2, United States Case Studies, Edited by T.D. O'Rourke and M.Hamada, Technical Report NCEER-92-0002.

Byrne, Peter M., (1991): "A Cyclic Shear-volume Coupling and Pore Pressure Model for Sand", Iwan, Proceedings: Second International Conference on Recent Advances in Geotechnical Engineering and Soil Dynamics, March, pp. 11 - 15, St. Louis, Missouri, Paper No. 1.24.

Houston, Sandra L., Houston, William N. and Padilla, J Manuel, (1987): "Microcomputer-aided Evaluation of Earthquake-induced Permanent Slope Displacements". Microcomputers in Civil Engineering 2.

Hynes, Mary E. and Franklin, Arley G., (1984): "Rationalizing the Seismic Coefficient Method", Geotechnical Laboratory, Department of the Army, Waterways Experiment Station, Corp. of Engineers, Vicksburg, Mississippi, July.

Iwan, W. D., (1967): "On a Class of Models for the Yielding Behaviors of Continuous and Composite System", Transaction of the ASME, September.

Larkin, T.J. and Marsh, E.J., (1982): "Two Dimensional Nonlinear Site Response Analysis", Proc. Pacific Conference on Earthquake Engineering, Vol. 3, pp. 217-227, Auckland, November.

Lee, Michael K. W. and Finn, W. D. Liam, (1978): "DESRA-2: Dynamic Effective Stress Response Analysis of Soil Deposit with Energy Transmitting Boundary Including Assessment of Liquefaction Potential", Department of Civil Engineering, University of British Columbia, Vancouver, Canada, June.

Newmark, Nathan M., (1959): "A Method of Computation for Structural Dynamics", Journal of the Engineering Mechanics Division, ASCE, Vol. 85, No. EM3, July.

Seed, H. Bolton and Harder, Leslie F., Jr., (1990): "SPT-based Analysis of Cyclic Pore Pressure Generation and Undrained Residual Strength", Memorial Symposium Proceedings, Volume 2, May, BiTech Publishers LTD.

Vaid, Yoginder P. and Finn, W.D. Liam, (1979): "Static Shear and Liquefaction Potential", Journal of the Geotechnical Engineering, ASCE, Vol. 105, No. GT10, October.

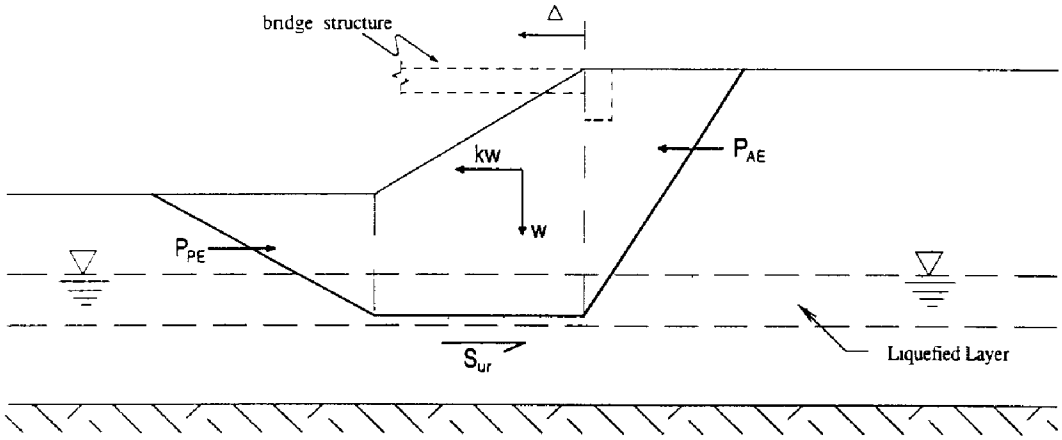

Fig. 1 Idealized Block Failure Mode of Bridge Approach Fill

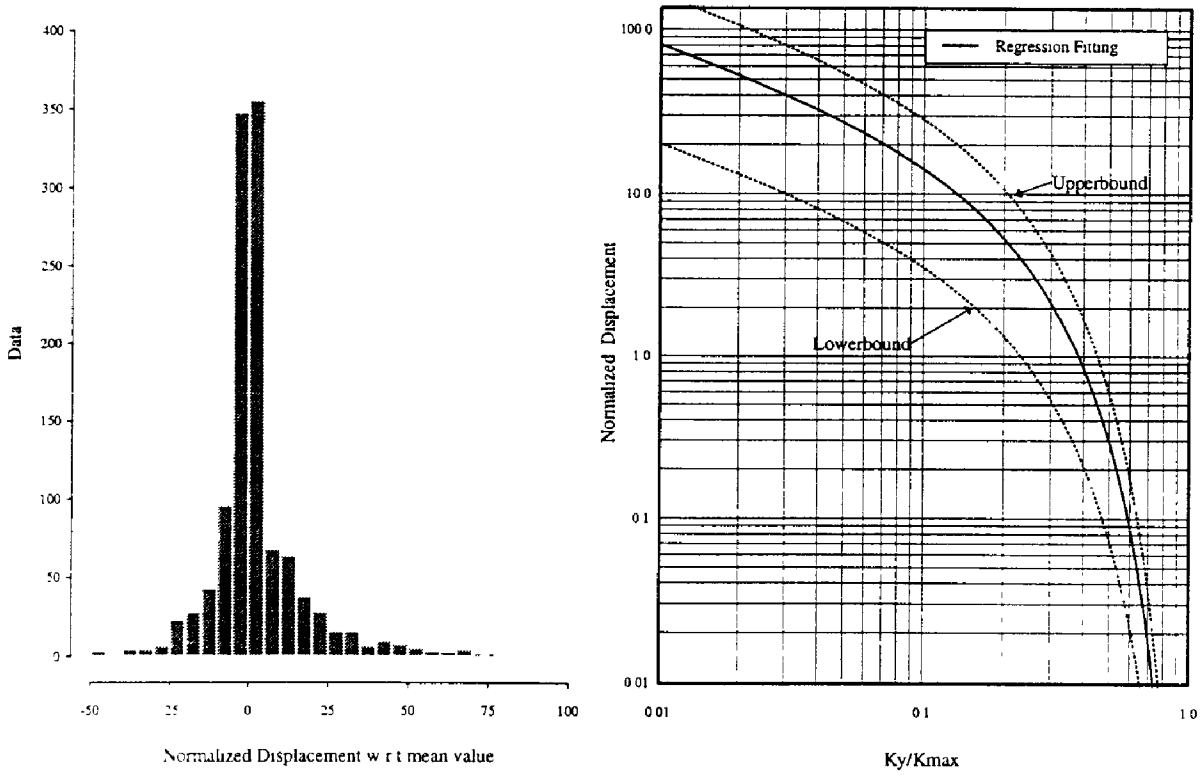

Fig. 2 Newmark Displacement Chart

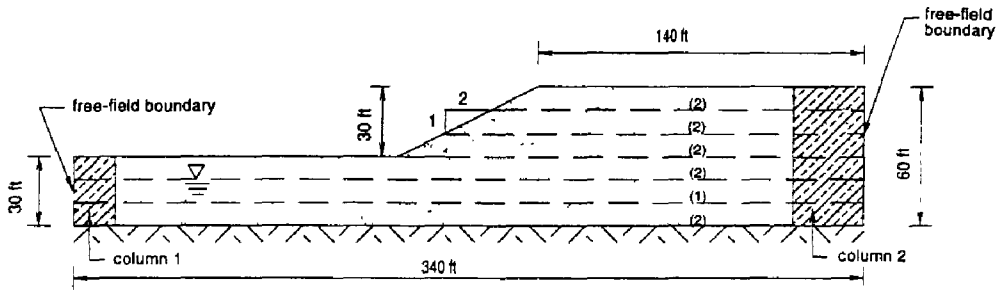

Summary of Material Properties of Nevada Sand

Layer	Relative Density	Possion's Ratio	Friction Angle	Coefficient of Permeability (m/s)	Residual Strength (psf)
1	40%	0.3	33	6.6×10^{-5}	200
2	60%	0.3	35	5.6×10^{-5}	700

Fig. 3 Configuration of an Idealized Embankment

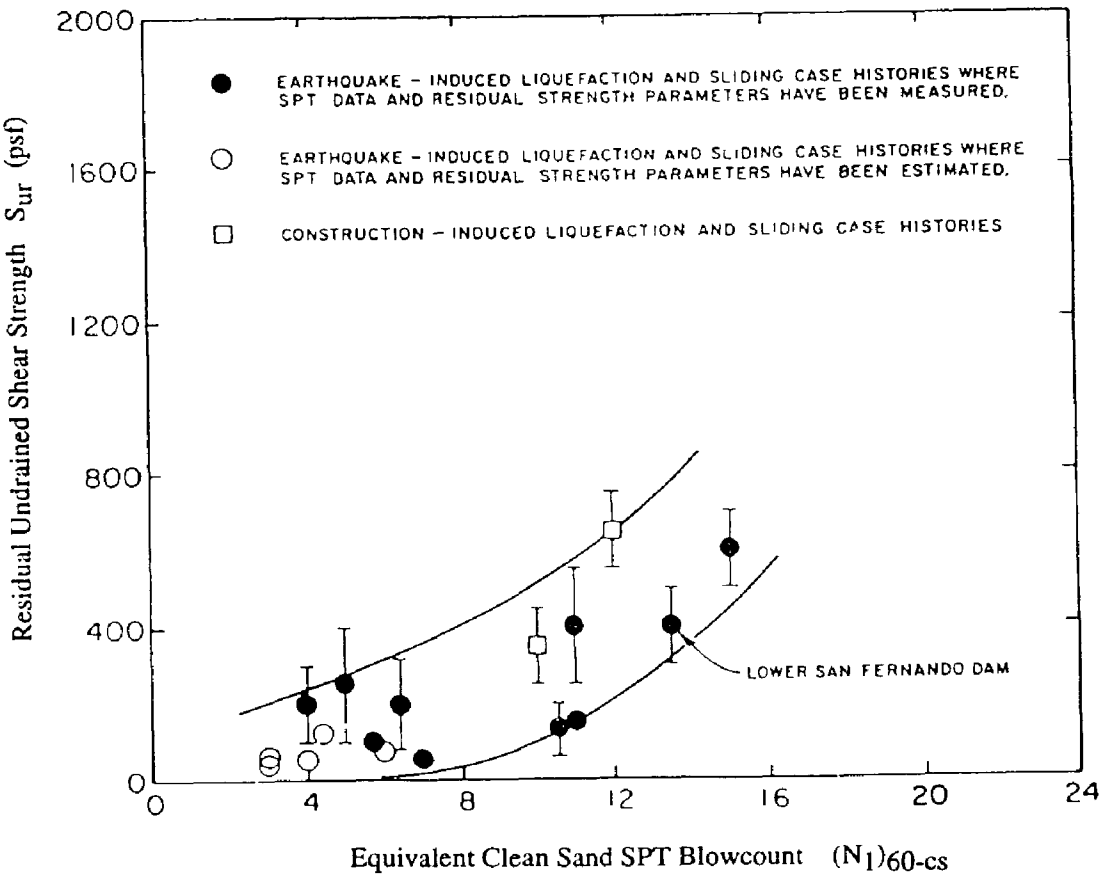

Fig. 4 Relationship Between Clean Sand Blowcount and Undrained Residual Strength from Case Studies

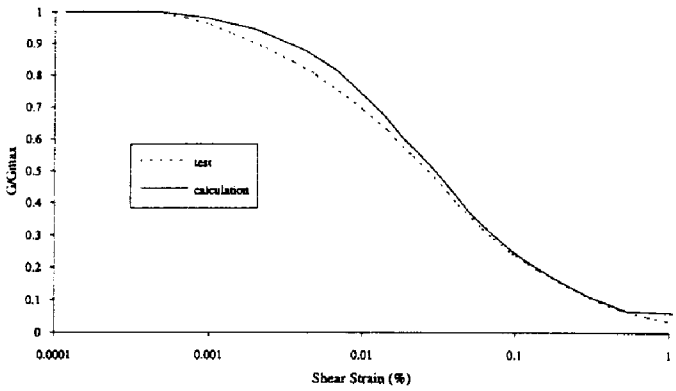

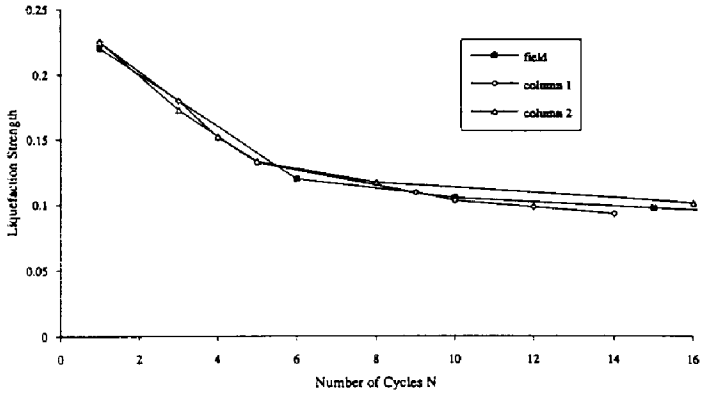

Fig. 5a Modeled versus Standard Shear Modulus-Shear Strain Curve

Fig. 5b Modeled versus Field Liquefaction Strengths

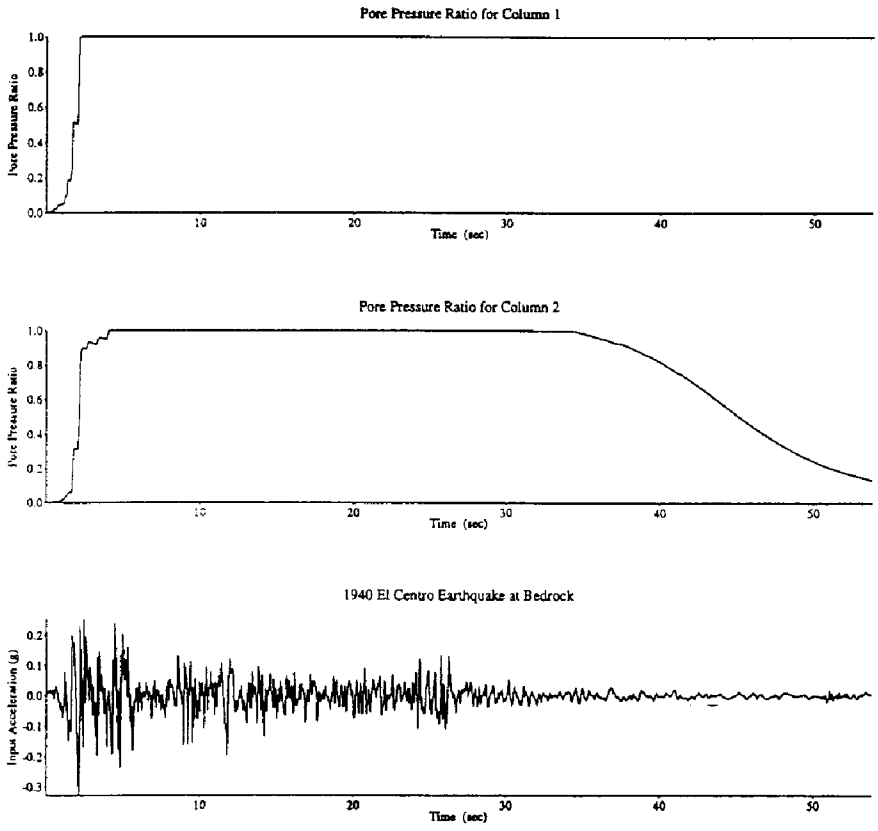

Fig. 6 DESRA-6 Liquefaction Evaluation

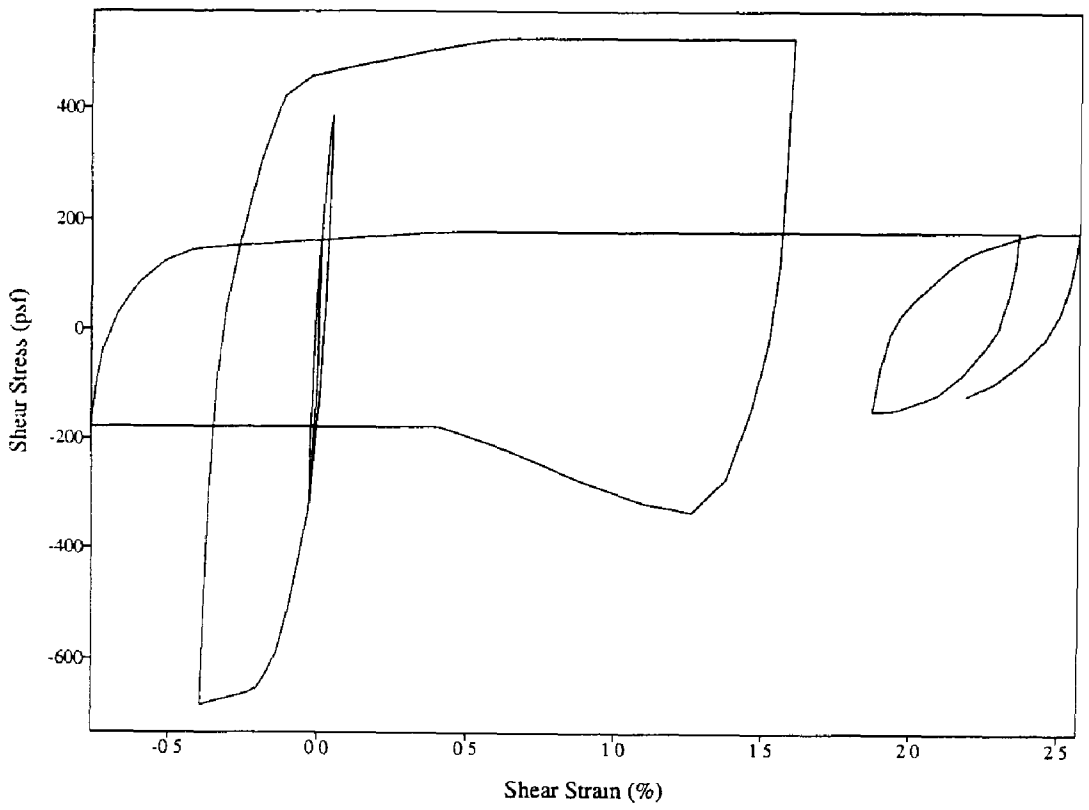

Fig. 7 Shear Stress vs. Shear Strain Time History (0 - 4 seconds) for Layer 1 (Column 2)

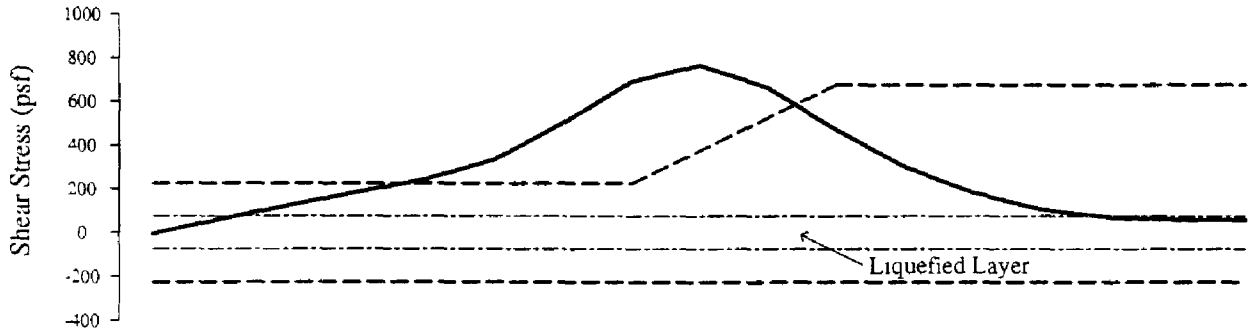

Fig. 8 Horizontal Static Shear Stress Distribution Due to Embankment Construction (Layer 1)

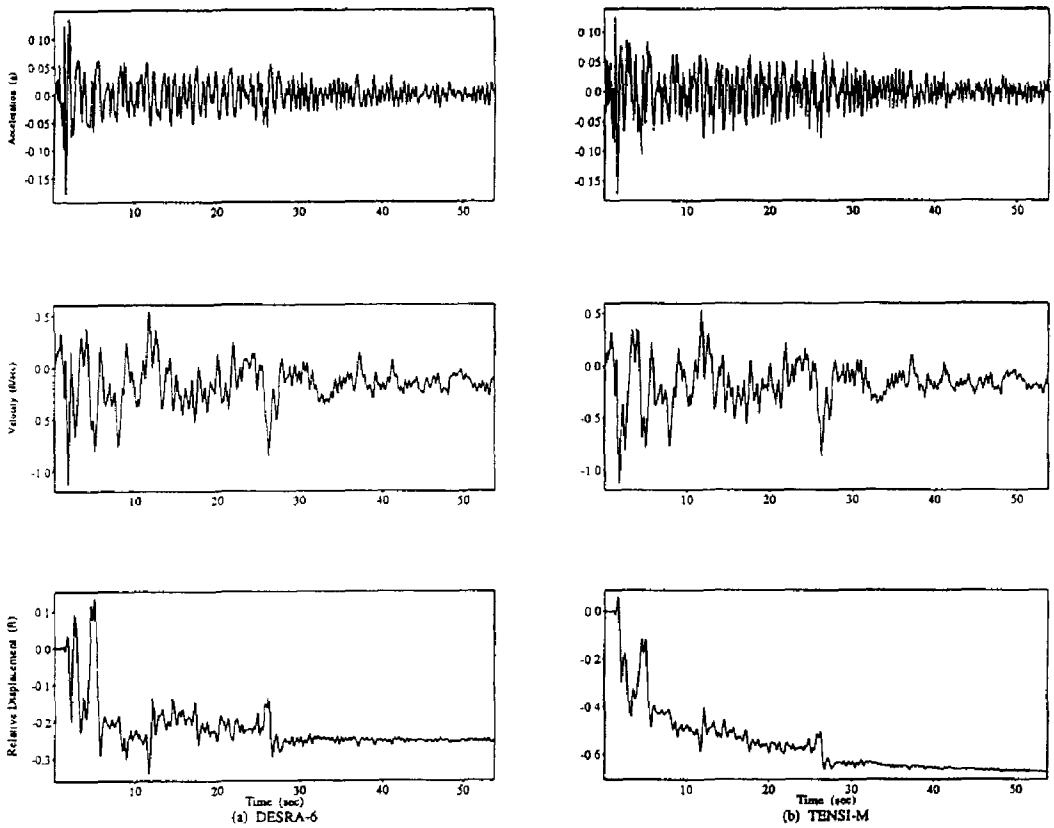

Fig. 9 Comparison of DESRA-6 and TENSI-M Results for Loose sand Layer - Column 1

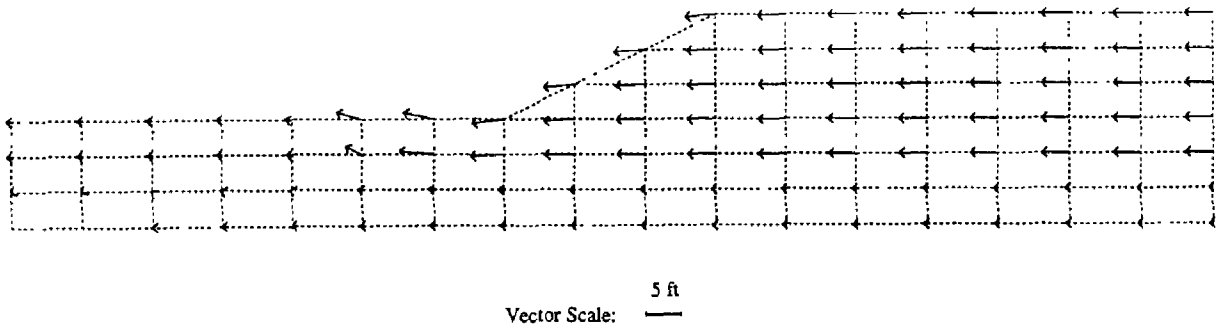

Fig. 10 Displacement Field Vectors

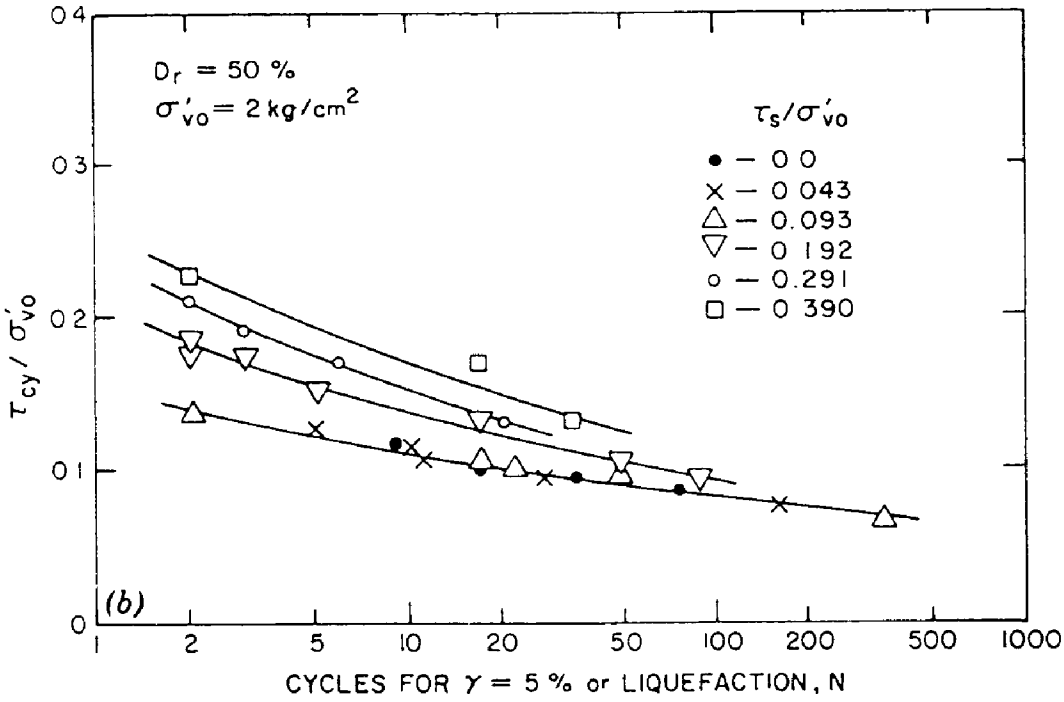

Fig. 11 Cyclic Shear Stress Required to Cause 5% Shear Strain (Loose Ottawa Sand, after Vaid and Finn, 1979)

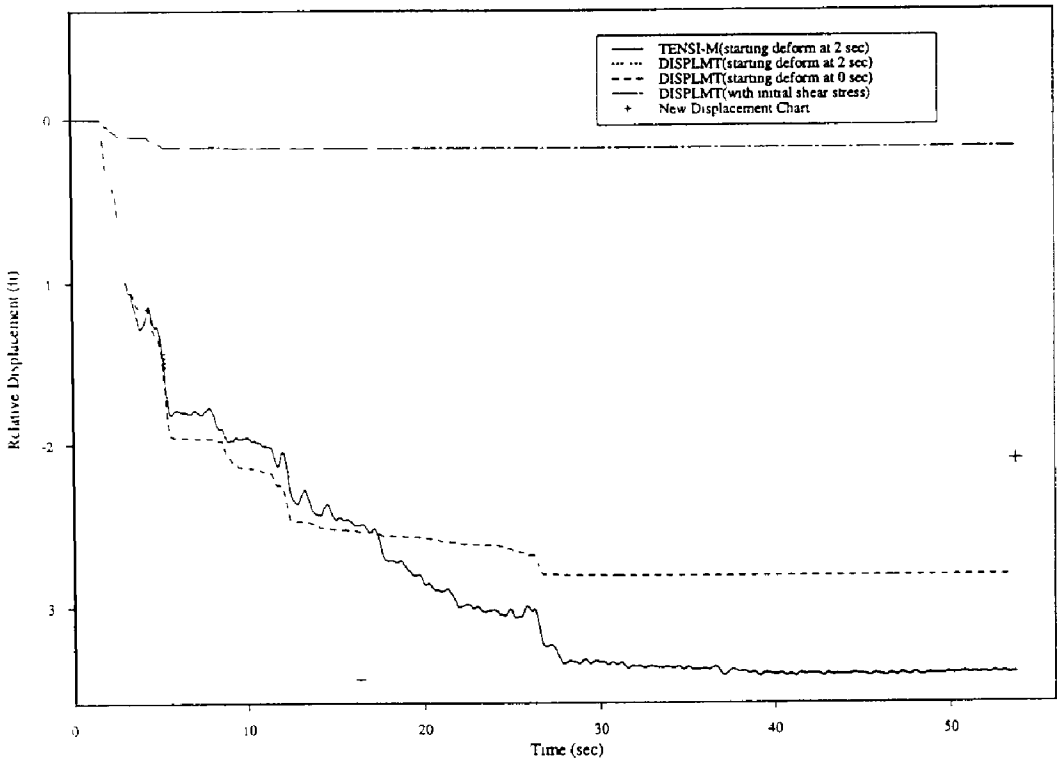

Fig. 12 Comparisons of Newmark Displacements for Liquefied Layer